Multi-Scale Modelling of Textile Reinforced Tissue Engineered Heart Valves

Scott E. Stapleton[1], Deepanshu Sodhani[2], Varun Raj[2], Ashish Sethi[2], Ricardo Moreira[3], Stefan Jockenhoevel[3], Petra Mela[3], and Stefanie Reese[2]

[1] Mechanical Engineering, University of Massachusetts Lowell, Lowell, MA, USA

[2] Institute of Applied Mechanics, RWTH Aachen University, Aachen, Germany

[3] Institute of Applied Medical Engineering, Helmholtz-Institute RWTH Aachen University, Aachen, Germany

Abstract*: Transcatheter aortic valve implantation of fibrin-based tissue engineered heart valves with a tubular leaflet construct have been developed as an alternative to invasive traditional surgical heart valve implantation, but currently need reinforcement to withstand pressures found in the aortic position. To increase valve strength, a PET textile reinforcement has been introduced to the fibrin scaffold. However, care must be taken when using a textile reinforcement. Increasing reinforcement may increase the strength, but also increases stiffness which can interfere with the functionality of the valve, prohibiting full valve closure. In order to predict the behavior of the valve, improve design, and eventually optimize valve performance by tailoring the textile reinforcement, a 4-tiered hierarchical multi-scale modelling framework has been created. The model includes an individual fiber scale model, two textile-level models, and a full heart valve model. Geometry generation based on microscopic images of the composite will be discussed, along with application of boundary conditions and loading application. Fitting the various material models based on homogenization of the smaller scale will be demonstrated. Finally, experimental validation and characterization at various scales will be discussed.*

Keywords*: Composites, Constitutive Model, Elasticity, Fabrics, Hyperelasticity, Implantable Medical Device, Tissue*

1. Introduction

Heart valve disease is a global health concern. Currently available heart prostheses are life-saving but present major limitations such as the need of a life-long anticoagulation therapy, the structural degeneration by calcification and the limited availability associated with mechanical valve, biological valve and homografts, respectively. Tissue-engineered heart valves have the potential to overcome these limitations providing a living prosthesis with remodeling and growing capabilities, physiological hemocompatibility and life-long duration.

In the recent past there is a considerable interest in developing artificial aortic tissue engineered heart valves (TEHVs). Tissue engineering (TE) of heart valves might overcome the well-known complications of contemporary devices such as the need for a life-long anticoagulation therapy in the case of mechanical prostheses (Padala et al., 2011; Pibarot & Dumesnil, 2009), the degeneration and therefore limited durability of the biological heart valves (Padala et al., 2011; Pibarot & Dumesnil, 2009) and the limited availability of homografts (Llames et al., 2012). The ultimate goal is to provide the patient with an implant produced with and by the patient's own cells, able to remodel and self-repair, with physiological haemocompatibility, biologically and mechanically equivalent to the native tissue. Different kinds of TEHVs are in development by various groups. One such TEHVs is being developed by the group at the Applied Medical Engineering institute of RWTH Aachen University (Weber et al., 2014).

Since experimental testing of different tissue-engineered heart valves can be extremely time-consuming and expensive, numerical models are desired to predict the effect of geometrical and material changes on performance. Hence, to predict the behavior of the artificial heart valve, which is basically a textile reinforced elastomeric composite, a well-known approach in the field of composites known as multi-scale modelling is employed. In this paper, we try to establish the validity of the approach for soft biological composites. Once the framework is set up, virtual testing and prediction of suitability of various soft biological composites in artificial heart valves can be developed into a very efficient tool for artificial heart valve development.

Various works on multi-scale modelling of heart valves exist in literature, where the problem at hand is tackled at organ, tissue, cell and molecular scales (Weinberg et al., 2010; Weinberg & Mofrad, 2007). In these approaches, the material characteristics of the higher scale is obtained from the lower scale, whereas the response of the underlying structure is often not accounted for clearly. (Argento et al., 2012) present an approach of mechanical characterization of the scaffolds for tissue engineered heart valves, by accounting for the effect of underlying scaffold structure, which is similar to the approach presented in this paper. In this work, the complex structure of the textile is divided into three simplified structural level models. The effective response obtained after conducting virtual experiments at the lower level model is used to represent the behavior at a higher level. In this manner the behavior of the textile embedded into the matrix is obtained. This effective response of the textile is then used to simulate the artificial textile reinforced heart valve under realistic loading conditions.

This paper is organized as follows. The structural multi-scale levels, along with a small introduction to the modelling approach is provided followed by an explanation of the constituents and model at each level. Finally, simulation is compared with an experiment for a valve made of silicone rather than tissue in a simulated circulatory system.

2. Method

The tube-in-stent valve design consists of a tubular construct sewn into a stent at three single attachment points and along a circumferential line at the annulus according to the single point attachment commissure (SPAC) technique (Goetz et al., 2002).

The current study uses silicone rather than engineered tissue for model validation to ease production and testing. The mechanical properties have been shown to be similar to that of engineered tissues (Martins et al., 2006), and serves as a good starting point for validating a computational model. One of the main benefits of using silicone initially is that there is less variability in material properties and geometry. This allows one to validate the model in a simpler fashion with less specimens before adding the complication of high variability.

A tubular knitted textile structure serves as reinforcement to strengthen and stiffen the valve (Moreira et al., 2014). The addition of the textile mesh adds a degree of complication to the modelling. The valves can be treated as a composite at the macro level, where the textile made by knitting multiple yarns (bundled fibers) is used as a scaffold on which the engineered tissues are grown (see Figure 1). Hence, to predict the behavior of a valve, one needs to understand the structural response of its constituents at different levels. Therefore, a multi-scale modelling approach is employed. The benefit of this approach is that individual components of the composite can be modelled by means of a simple material model which can be characterized using simple experiments. The effective response of the material over different scales can then be obtained from virtual experiments.

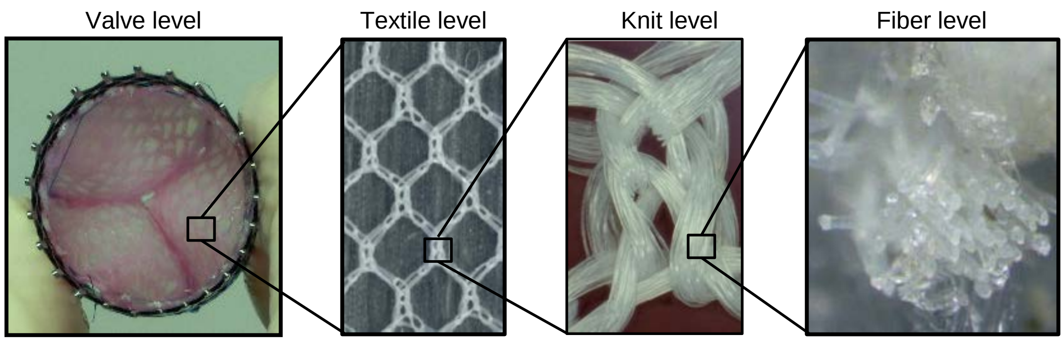

Figure 1. Structural levels/scales considered for the textile-reinforced tissue engineered heart valve.

The following sections will first outline some aspects of the finite element modelling, emphasizing characteristics of the models that is common for all models. Finally, each level will be examined individually. At each level, the constituents will be identified and the means of characterization, whether it be through experiments or virtual experiments at the smaller scale, will be outlined. Finally, the validation experiment on the valve will be described.

2.1 Finite Element Modelling

A summary of the models and the constituents at each level is shown in Figure 2. All the finite element (FE) models were created using the commercial software Abaqus (*Abaqus User's Manual, Version 6.14,* n.d.). The elements used are C3D4 (linear tetrahedral) and C3D8R (eight-noded brick elements with reduced integration and enhanced hourglass stiffness) depending on the structural model in consideration. All the structural models were simulated using the implicit (standard) solver of Abaqus, whereas the heart valve model was solved using the explicit solver. Only the material models built into Abaqus were used in this work.

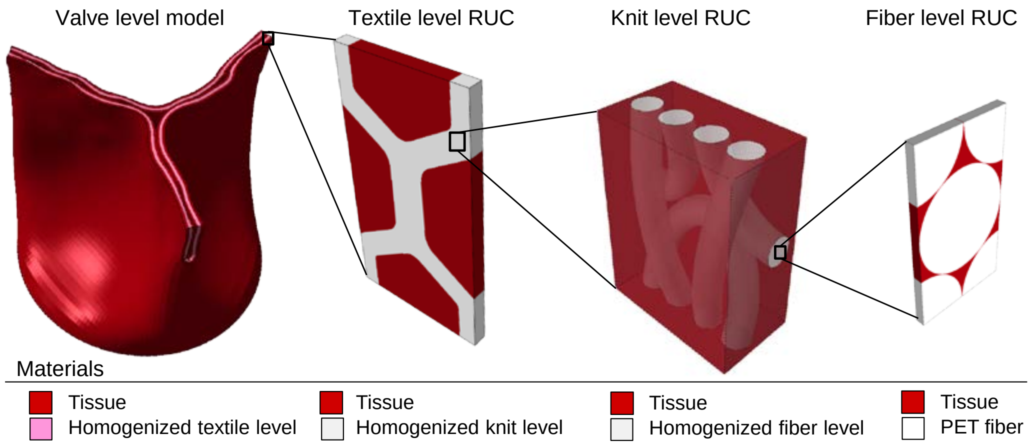

Figure 2. Multiple levels are each modeled, with the smaller levels represented with repeating unit cells (RUCs), with the constituents for each level listed below.

The micro-structure has been simplified and divided into four levels. The schematic representation of the different levels used in multi-scale modelling is shown in Figure 2. The modelling approach of repeating unit cells (RUC) (Hassani & Hinton, 1998) was implemented at textile, knit and fiber levels. A unit cell, when repeated in all or specified directions, represents the micro-structure, i.e. the structure is periodic along the pre-defined directions. Virtual experiments are conducted at a lower level RUC which then produces the effective material response. This effective material response was subsequently fitted by another material model used to represent the behavior of the internal structure within the RUC at a higher level. The same procedure was repeated until all the scales under investigation were accounted for. This approach is often referred to as hierarchical multi-scaling (Bednarcyk et al., 2015). For the three smaller levels (fiber, knit, and textile), displacement-based periodic boundary conditions (PBCs) were used for the prediction of effective material response (Bednarcyk et al., 2015). Silicone matrix and the PET fibers were characterized using experimental results, whereas virtual experiments conducted on the RUC are used to characterize the material properties of the internal structure in a higher level RUC. The response of the RUC was homogenized through a volume-averaging homogenization, and was used to fit a material model at the higher scale.

2.2 Fiber Level

The fiber level represents the micro-structure of the yarn. 24 PET fibers with a diameter of 17 μm are bundled together as a yarn. Within a yarn, it was assumed that all the fibers are aligned in the direction of the yarn. Hence, a hexagonal dense packing (HDP) RUC was used to represent the yarns. Yarns were represented in the knit level model using a circular cross-section, with a volume fraction of 90%. Therefore, the HDP RUC is modelled with a volume fraction of 90%.

2.2.1 Constituents

At the fiber level, the fibers and matrix were modelled as linear-elastic, isotropic materials. The elastic parameters were obtained by fitting the initial linear portion of experimentally-determined stress-strain curves as shown in Figure 3. The silicone matrix was characterized using tensile tests. The specimens had a gauge length of 31.28 mm, a width of 6.35 mm, and a nominal thickness of around 1.15 mm. The specimens were preloaded with 0.5 N, and stretched at 3 mm/min until failure. The engineering stress vs. stretch is plotted in Figure 3. As can be seen, silicone has a hyperelastic material response, which undergoes softening under cyclic loading representing the Mullins' effect. Since the heart valve is subjected to cyclic fatigue loading, the silicone matrix was characterized only by the unloading curve of the last cycle. The silicone matrix (Elastosil) was found to have a modulus of E=0.7323 MPa and assumed a Poisson's ratio of ν=0.49, which was fit from the experimental data.

The PET fiber material parameters were obtained by using experimental data found in literature (Lechat et al., 2010). This stress vs strain curve is from a tensile test on a single PET fiber. The curve appears to be linear initially (except for an initial non-linear period which is assumed by the authors to be remnants of the load transfer in the experimental set-up rather than actual material behavior) until it became plastic. Since plasticity is not included in the present model, only linear elasticity is considered where E=10.259 GPa was fitted from the experimental data and ν=0.35 was assumed.

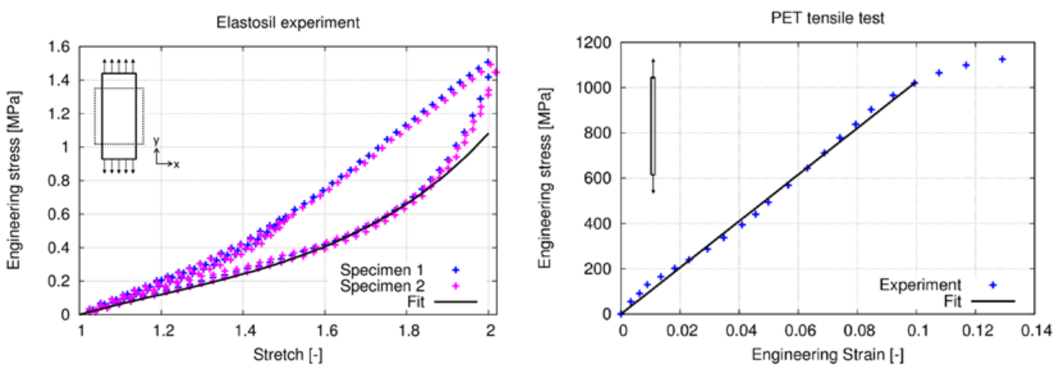

Figure 3. Experimentally determined stress-strain curves along with fits for the constituents at the fiber level for Elastosil and PET fibers (Lechat et al., 2010).

2.2.2 Homogenization

The homogenized material response from the fiber level was used to represent the yarn in the knit level. The response was used to fit a linear elastic transversely isotropic model. The material properties of the yarn, used in the knit level RUC, were modelled using a transversely isotropic material law. Transverse isotropy is a special case of orthotropy, where the material has the same properties in one plane and different properties in the direction normal to this plane. These materials can be described by five independent elastic constants. By convention, the five elastic constants in transversely isotropic constitutive equations are the Young's modulus and Poisson's ratio in the symmetry plane, E_p and ν_p, the Young's modulus and Poisson's ratio in the normal direction, E_n and ν_{np}, and the shear modulus μ_{np}. Considering the out of plane direction to be the z-direction, the compliance matrix takes the form:

$$\begin{bmatrix} \epsilon_{xx} \\ \epsilon_{yy} \\ \epsilon_{zz} \\ 2\epsilon_{yz} \\ 2\epsilon_{xz} \\ 2\epsilon_{xy} \end{bmatrix} = \begin{bmatrix} \frac{1}{E_p} & -\frac{\nu_p}{E_p} & -\frac{\nu_{np}}{E_n} & 0 & 0 & 0 \\ -\frac{\nu_p}{E_p} & \frac{1}{E_p} & -\frac{\nu_{np}}{E_n} & 0 & 0 & 0 \\ -\frac{\nu_{np}}{E_p} & -\frac{\nu_{np}}{E_p} & \frac{1}{E_p} & 0 & 0 & 0 \\ 0 & 0 & 0 & \frac{1}{\mu_{np}} & 0 & 0 \\ 0 & 0 & 0 & 0 & \frac{1}{\mu_{np}} & 0 \\ 0 & 0 & 0 & 0 & 0 & \frac{1+\nu_p}{E_p} \end{bmatrix} \begin{bmatrix} \sigma_{xx} \\ \sigma_{yy} \\ \sigma_{zz} \\ \tau_{yz} \\ \tau_{xz} \\ \tau_{xy} \end{bmatrix}$$

A far-field strain of 1\% was applied to the RUC in three uni-axial strain and three shear deformation modes in order to fully populate the elasticity tensor (see (D Sodhani et al., 2015)). Each component of strain was applied with all other strain components set to zero, and the slope of the response in different directions was used to find the corresponding row in the elasticity tensor. This was repeated for each of the six strain components to obtain the fully-populated elasticity tensor. The material parameters, Young's modulus, shear modulus and the Poisson's ratio, were obtained from the compliance tensor (which is the inverse of stiffness tensor) as follows: E_n=9233.01 MPa, E_p=346.43, MPa, ν_p=0.417, ν_{np}=0.013, μ_{np}=13.72 MPa, and μ_p=122.33 MPa.

2.3 Knit Level

Modelling a complex knit pattern can be computationally challenging and expensive. Even though the kitted textile has a repetitive pattern, it is difficult to identify a consistent path along which the yarns are knit. Hence, it was found necessary to simplify the knit for computationally efficient modelling. The simplified knit pattern has to account for the continuous load transfer within the yarns from one knit to another and also the locking of yarn alignment in loading direction due to the looping structure of the knit. Therefore, in this work, the complex knits were approximated by a simplified knit pattern with a volume fraction of 19%.

2.3.1 Constituents

Two constituents were considered in the knit level: homogenized fiber level material and silicon matrix. The homogenized fiber level material parameters are explained in Section 2.2.2. The silicon at this level and all higher levels was modeled using the Arruda Boyce model (Arruda & Boyce, 1993) which is an isotropic hyperelastic constitutive model used to describe the mechanical behavior of rubber-like and other polymeric substances. This model is based on the statistical mechanics of a material with a cubic representative volume element containing eight chains along the diagonal directions. The material is assumed to be incompressible. The strain energy density function for the incompressible (Arruda & Boyce, 1993) model is given by

$$W = N k_B \theta \sqrt{n}\left[\beta\lambda_{chain} - \sqrt{n}\ln\frac{\sinh\beta}{\beta}\right]$$

where n is the number of chain segments, k_B is the Boltzmann's constant, θ is the temperature in Kelvin and N is the number of chains/density of chains in the network of cross-linked polymers, and

$$\lambda_{chain} = \sqrt{\frac{I_1}{3}};\ \beta = L^{-1}\left(\frac{\lambda_{chain}}{\sqrt{n}}\right);\ \mu_{ab} = Nk_B\theta$$

where λ_{chain} represents the stretch of a chain, I_1 is the first invariant of the right Cauchy-Green deformation tensor, $L^{-1}(x)$ is the inverse Langevin function, and μ_{ab} is the shear modulus obtained by fitting the experimental results. By considering the full curve in Figure 3, the constants μ_{ab} and n were found to be 0.0862 MPa and 1.1762 respectively through curve fitting.

2.3.2 Homogenization

To fit the response at the knit level, Fung's orthotropic hyperelastic material model (Fung et al., 1979) was utilized. Various other orthotropic/anisotropic hyperelastic material models such as the ones suggested by (Ehret & Itskov, 2007; Gasser et al., 2006; Holzapfel, 2004; Holzapfel & Gasser, 2001; Reese et al., 2001) could also be used to represent orthotropic/anisotropic material response. The generalized Fung strain energy potential in Abaqus is based on the two-dimensional exponential form proposed by (Fung et al., 1979), which was suitably generalized to arbitrary three-dimensional states using (Humphrey, 1995). It has the form

$$W = \frac{c}{2}(e^Q - 1) + \frac{K}{2}\left(\frac{J^2 - 1}{2} - \ln J\right)$$

where

$$Q = \boldsymbol{E}:\boldsymbol{B}:\boldsymbol{E}$$

$\boldsymbol{B}$ is a dimensionless symmetric fourth-order tensor of anisotropic material constants and $\mathbf{E}$ represents the Green-Lagrange strain tensor. The orthotropic form of the generalized Fung model with eleven independent variables is used in this work. The Voigt notation is denoted by **B,** given by

$$\mathbf{B} = \begin{bmatrix} \mathrm{b}_1 & \mathrm{b}_7 & \mathrm{b}_8 & 0 & 0 & 0 \\ \mathrm{b}_7 & \mathrm{b}_2 & \mathrm{b}_9 & 0 & 0 & 0 \\ \mathrm{b}_8 & b_9 & b_3 & 0 & 0 & 0 \\ 0 & 0 & 0 & b_4 & 0 & 0 \\ 0 & 0 & 0 & 0 & b_5 & 0 \\ 0 & 0 & 0 & 0 & 0 & b_6 \end{bmatrix}$$

Virtual tensile and pure shear tests were carried out at the knit level RUC for a far field strain of 25%. The material response was then fitted with the orthotropic hyperelastic Fung's model, one row of **B** at a time. The effective material response and the material fit are shown in Figure 4. The constants c and K were found to be 1.008 and 4.163 MPa, respectively. The nine independent parameters ($b_1 - b_9$) were found to be 1.939, 33.412, 0.779, 14.649, 6.039, 11.409, 2.591, 0.229, and 1.319 respectively.

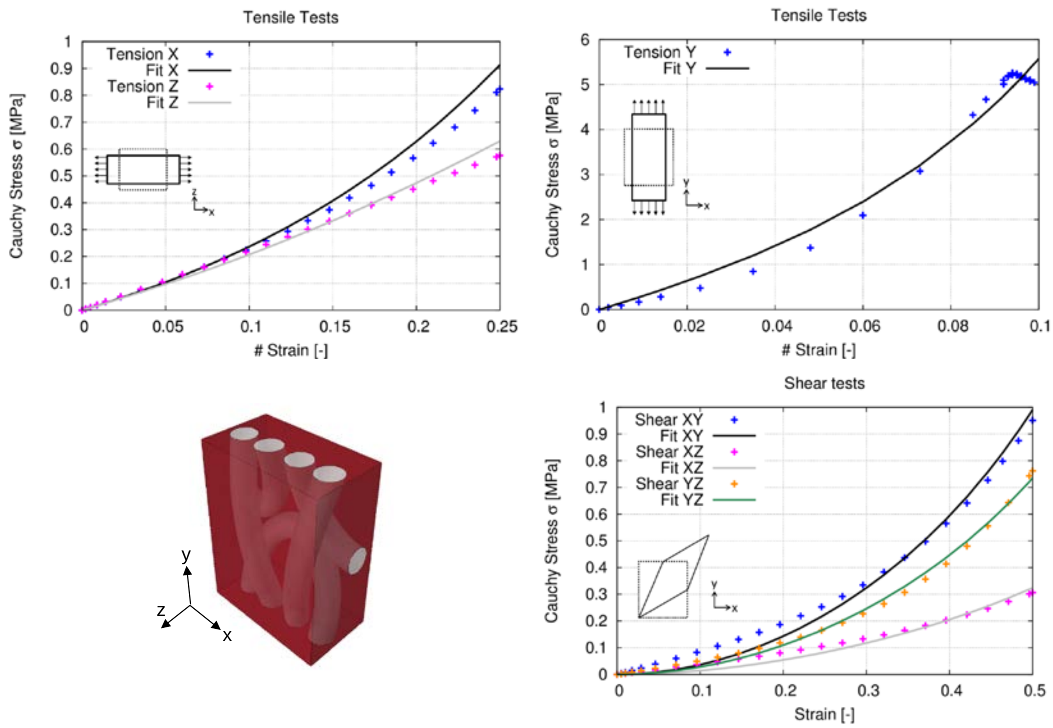

Figure 4. Results of various RVE loading cases along with the associated fit of the knit level which was used as a constituent at the textile level.

2.4 Textile Level

Structurally, the textile level represents a honeycomb pattern. The honeycomb pattern should provide the textile with equivalent in-plane stiffness. This was modelled using an RUC with an internal structure of volume fraction 36.67%. Orthotropic Fung's hyperelastic material model is used to represent the internal structure in the RUC, and the matrix is modelled as incompressible hyperelastic material. The homogenized knit level response is smeared over the internal structure using local orientations. Homogenized material response from this level is used to represent the center layer in the heart valve model.

2.4.1 Constituents

The textile level model consisted of silicone matrix as described in Section 2.3.1 and the homogenized knit level material as described in Section 2.3.2.

2.4.2 Homogenization

The effective material response of the textile level RUC was obtained by subjecting it to a far field tensile strain of 50% and pure shear strain of 25%. These were then fitted with the orthotropic hyperelastic Fung's model as done for the knit level (see Figure 5). A monte-carlo type optimization algorithm was used to fit the curves in each direction. As expected, one can observe that the RUC has comparable stiffness in X and Y directions, which is the effect of the honeycomb structure. A shear test was carried out only in the XY plane to obtain the b_4 parameter. Parameters b_5 and b_6 were assumed to be the same as b_4. The parameters c and K were found to be 1.1635 and 2.000 MPa, respectively. Additionally, $b_1 - b_9$ were found to be 1.1957, 1.2917, 0.6059, 12.5, 12.5, 12.5, 0.0828, 0.1396, and 0.1493 respectively.

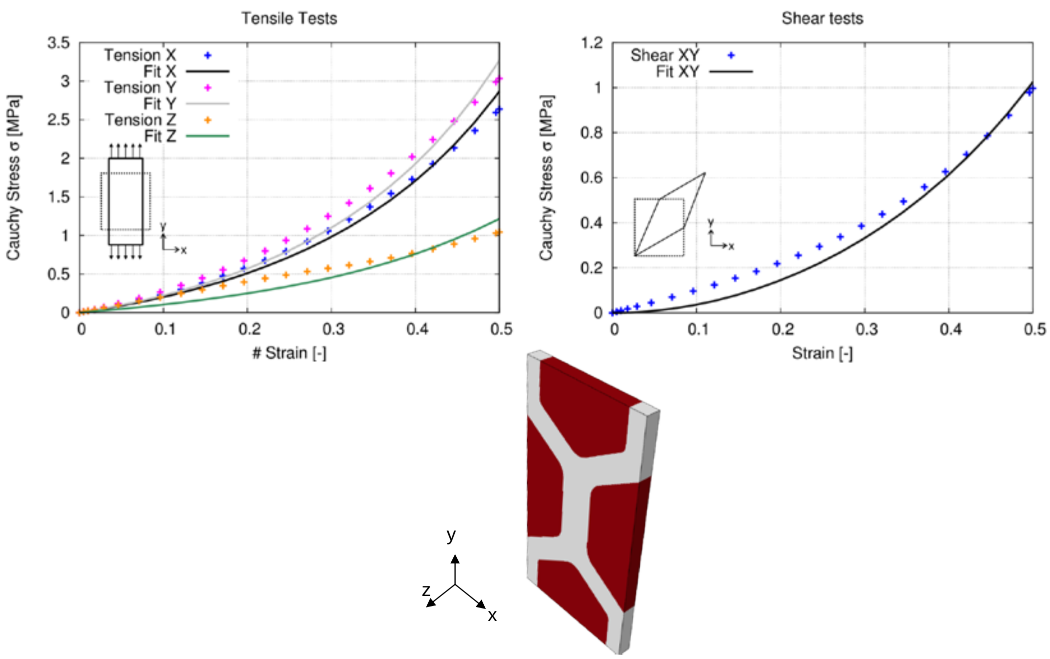

Figure 5. Results of various RVE loading cases along with the associated fit for the textile level which was used as a constituent at the valve level.

2.5 Valve Level

Finally, the entire valve was modelled to emulate the opening and closing of the valve in the body. The results of the simulation were compared with images of a valve experiment for a textile-reinforced valve with silicone instead of tissue.

2.5.1 Constituents

The heart valve consists of two constituents: pure tissue and a textile-reinforced tissue layer. The textile reinforced layer is modelled by the orthotropic hyperelastic Fung's model obtained from the textile level model. The outer and the inner layers are considered to be pure matrix (silicone or engineered tissue) layers and are modelled using the isotropic hyperelastic Arruda Boyce material model as discussed in the knit level section.

2.5.2 Experiment

The simulations in the paper are based on the tubular valve construct as shown in Figure 1 (see also (Stapleton et al., 2015)). The diameter of the heart valve was 23 mm with a thickness of 0.7 mm and a height of 18 mm. A simulation was carried out on the initial tubular construct to achieve the geometry of the sutured heart valve. The deformed geometry was then extracted from the output file to obtain a stress free initial sutured configuration. Displacement boundary conditions are summarized as in Figure 6. The three constitutive layers along the thickness: tissue, a layer with textile reinforcement, and another tissue layer were modelled with one element (i.e. single integration point) through the thickness as can be seen in Figure 6.

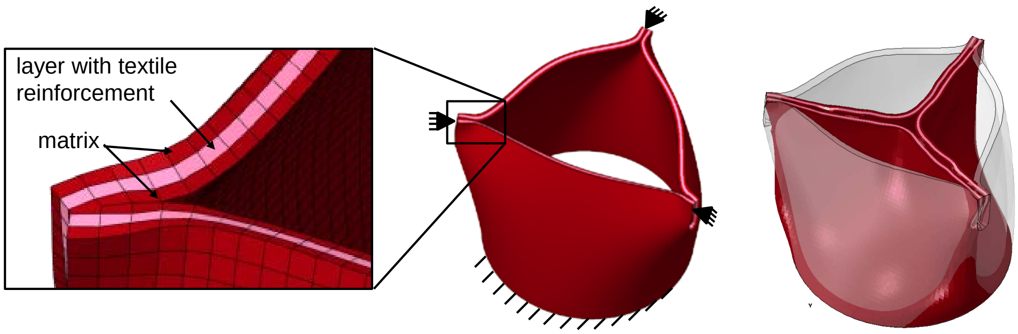

Figure 6. Illustration showing mesh details, boundary conditions, and open/closed configuration.

Aortic and ventricular surface pressures were applied to simulate the cardiac cycle while keeping the suture points and the base of the heart valve fixed. The experimental aortic and the ventricular pressure which are similar to the cardiac cycle (Figure 7) were fitted by a Fourier and applied as a periodic change in amplitude within Abaqus (*Abaqus User's Manual, Version 6.14*, n.d.) as shown in Figure 7.

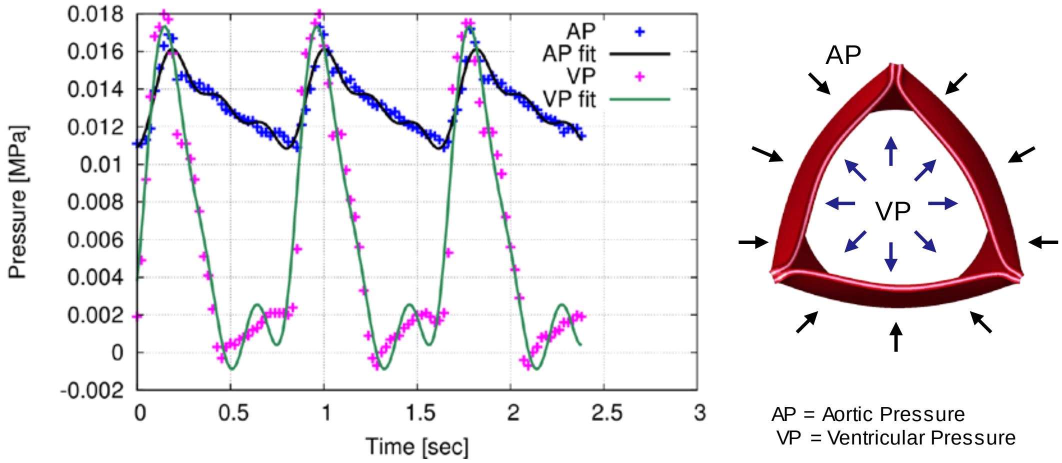

Figure 7. Flow is simulated in the heart valve by applying inner (VP) and outer (AP) pressures in a cyclic manner on the sutured heart valve.

For the validation, a silicon tubular construct reinforced with a PET textile was created and sutured to a stent. The valve was placed in a custom-made bio-reactor positioned in an incubator. With the use of actuators and membranes, the bio-reactor was able to mimic the stroke flow loop between the ventricle and the aorta using aortic flow and pressure conditions according to ISO 5840-3 i.e., cardiac output of 5L/min, 100 mmHg mean aortic pressure and 70 bpm (beats per minute) frequency. The pressures was measured by pressure transducers positioned immediately upstream and downstream from the valves. The instantaneous flow is measured by a flow meter positioned downstream from the valves, and images of the valve were taken during the experiment.

3. Validation

To validate the results of the simulation with the experimental set-up, the open areas of the experimental and simulated heart valve were compared. An image processing method was used to acquire the percentage of the open cross-section of the heart valve during the systole phase of the cardiac cycle to its initial cross-section. Figure 8 shows snapshots of the experimental heart valve over the cardiac cycle in comparison with the snapshot of the simulation at the same time step along with a plot of the open area over time. From the comparison, it can be observed that the percentage opening of the experiment and the simulation during the systole phase of the cardiac cycle are almost the same, whereas in the diastole phase, the simulated heart valve does not close completely due to the reasons mentioned earlier. In the opinion of the authors, the current validation method, though not the most accurate, serves to validate the approach used to simulate the behavior of the textile reinforced artificial heart valve.

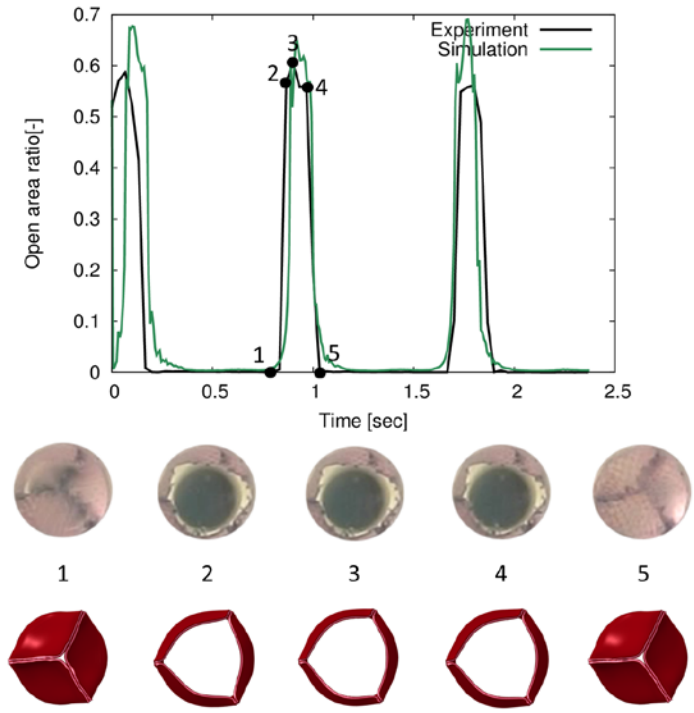

Figure 8. Comparison of the opening area of the heart valve in the bioreactor and for the simulated heart valve.

4. Conclusion

The goal of the current study was to show that competence of the multi-scale modelling approach to predict the behavior of textile reinforced aortic heart valves, has been achieved. First, the complex structure of the heart valve was reduced to simplified structural models at different scales. Then, different relatively simple material models available in a Abaqus were introduced. Repeating unit cells (RUCs) of these simplified structural models were then meshed to obtain a finite element (FE) model. These were then subjected to periodic boundary conditions and loaded using far field strain to obtain an effective material response. The effective material response was then fitted using the appropriate material models.

A macro FE model was constructed for the heart valve. The model was divided into three zones over the thickness. The outer layer was modelled as pure silicone matrix, whereas the material properties of the textile layer were derived from the hierarchical multi-scaling approach. Dynamic simulation of the heart valve was carried out, where, in the first step the heart valve was sutured to avoid excessive distortion at one point. In the next step, ventricular and aortic pressures were applied on the inner and the outer surface of the heart valve. The obtained deformation pattern of the heart valve and percentage open area of the cross-section during systole and diastole phase of the cardiac cycle are in good agreement with the experimental results.

Further, the closing response of the heart valve needs to be improved, which can be achieved by mesh refinement over the thickness of the heart valve and a modified multi-scale modelling approach. Blood flow simulation using fluid-structure interaction also needs to be carried out to realistically simulate the cardiac cycle and analyze the flow volume through the valve. For more efficient modelling of the TEHV, a material model accounting for extra-cellular fiber (elastin and collagen) alignment within the matrix under cyclic loading during cultivation needs to be developed. To make the approach more reliable and robust further investigations are needed to quantify the deviation of the final result due to the change in volume fraction of individual structural levels, such that the modelling is faithful to the overall volume fraction of the heart valve. Also, further investigations are needed to determine the effect of different knit patterns in the knit level model on the overall results.

5. Acknowledgements

This research was partially funded by the Integrated Interdisciplinary Institute of Technology for Medicine of RWTH Aachen University, through the Seed-Fund SF-14-04-08, ``Hybrid scaffold for a transcatheter tissue-engineered aortic valve". Additional funding was provided by the People Programme (Marie Curie Actions) of the European Union's Seventh Framework Programme FP7/2007-2013/ under REA grant agreement °317512. The authors would additionally like to thank Bertram Stier for his script to apply periodic boundary conditions and for helpful discussion and support.

6. References

Abaqus User's Manual, Version 6.14. (n.d.). Providence, RI: Dassault Systémes Simulia Corp.

Argento, G., Simonet, M., Oomens, C.W.J. & Baaijens, F.P.T. (2012). Multi-scale mechanical characterization of scaffolds for heart valve tissue engineering. *Journal of Biomechanics 45*(16): 2893–2898.

Arruda, E.M. & Boyce, M.C. (1993). A three-dimensional constitutive model for the large stretch behavior of rubber elastic materials. *Journal of the Mechanics and Physics of Solids 41*(2): 389–412.

Bednarcyk, B.A., Stier, B., Simon, J.-W., Reese, S. & Pineda, E.J. (2015). Meso- and micro-scale modeling of damage in plain weave composites. *Composite Structures 121*: 258–270.

D Sodhani, B Stier & S Reese. (2015). Evaluating the simulation of ideal filler reinforced elastomers using a full field modelling approach. In *Constitutive Models for Rubbers IX* (Vols. 1-0). CRC Press. Retrieved from http://www.crcnetbase.com/doi/abs/10.1201/b18701-56

Ehret, A.E. & Itskov, M. (2007). A polyconvex hyperelastic model for fiber-reinforced materials in application to soft tissues. *Journal of Materials Science 42*(21): 8853–8863.

Fung, Y.C., Fronek, K. & Patitucci, P. (1979). Pseudoelasticity of arteries and the choice of its mathematical expression. *The American Journal of Physiology 237*(5): H620–631.

Gasser, T.C., Ogden, R.W. & Holzapfel, G.A. (2006). Hyperelastic modelling of arterial layers with distributed collagen fibre orientations. *Journal of The Royal Society Interface 3*(6): 15–35.

Goetz, W.A., Lim, H.-S., Lansac, E., Weber, P.A. & Duran, C.M.G. (2002). A temporarily stented, autologous pericardial aortic valve prosthesis. *The Journal of Heart Valve Disease 11*(5): 696–702.

Hassani, B. & Hinton, E. (1998). A review of homogenization and topology optimization I—homogenization theory for media with periodic structure. *Computers & Structures 69*(6): 707–717.

Holzapfel, G.A. (2004). Computational Biomechanics of Soft Biological Tissue. In *Encyclopedia of Computational Mechanics*. John Wiley & Sons, Ltd. Retrieved from http://onlinelibrary.wiley.com/doi/10.1002/0470091355.ecm041/abstract

Holzapfel, G.A. & Gasser, T.C. (2001). A viscoelastic model for fiber-reinforced composites at finite strains: Continuum basis, computational aspects and applications. *Computer Methods in Applied Mechanics and Engineering 190*(34): 4379–4403.

Humphrey, J.D. (1995). Mechanics of the arterial wall: review and directions. *Critical Reviews in Biomedical Engineering 23*(1-2): 1–162.

Lechat, C., Bunsell, A.R. & Davies, P. (2010). Tensile and creep behaviour of polyethylene terephthalate and polyethylene naphthalate fibres. *Journal of Materials Science 46*(2): 528–533.

Llames, S., García, E., Hernández, J.O. & Meana, Á. (2012). Tissue Bioengineering and Artificial Organs. In C. López-Larrea, A. L.-V. MD & B. Suárez-Álvarez (eds.), *Stem Cell Transplantation*. Springer US. Retrieved from http://link.springer.com/chapter/10.1007/978-1-4614-2098-9_20

Martins, P. a. L.S., Natal Jorge, R.M. & Ferreira, A.J.M. (2006). A Comparative Study of Several Material Models for Prediction of Hyperelastic Properties: Application to Silicone-Rubber and Soft Tissues. *Strain 42*(3): 135–147.

Moreira, R., Velz, T., Alves, N., Gesche, V.N., Malischewski, A., Schmitz-Rode, T., … Mela, P. (2014). Tissue-Engineered Heart Valve with a Tubular Leaflet Design for Minimally Invasive Transcatheter Implantation. *Tissue Engineering. Part C, Methods*.

Padala, M., Keeling, W.B., Guyton, R.A. & Thourani, V.H. (2011). Innovations in therapies for heart valve disease. *Circulation Journal: Official Journal of the Japanese Circulation Society 75*(5): 1028–1041.

Pibarot, P. & Dumesnil, J.G. (2009). Prosthetic Heart Valves Selection of the Optimal Prosthesis and Long-Term Management. *Circulation 119*(7): 1034–1048.

Reese, S., Raible, T. & Wriggers, P. (2001). Finite element modelling of orthotropic material behaviour in pneumatic membranes. *International Journal of Solids and Structures 38*(52): 9525–9544.

Stapleton, S.E., Moreira, R., Jockenhoevel, S., Mela, P. & Reese, S. (2015). Effect of reinforcement volume fraction and orientation on a hybrid tissue engineered aortic heart valve with a tubular leaflet design. *Advanced Modeling and Simulation in Engineering Sciences 2*(1): 21.

Weber, M., Heta, E., Moreira, R., Gesche, V.N., Schermer, T., Frese, J., … Mela, P. (2014). Tissue-engineered fibrin-based heart valve with a tubular leaflet design. *Tissue Engineering. Part C, Methods 20*(4): 265–275.

Weinberg, E.J. & Mofrad, M.R.K. (2007). Transient, Three-dimensional, Multiscale Simulations of the Human Aortic Valve. *Cardiovascular Engineering 7*(4): 140–155.

Weinberg, E.J., Shahmirzadi, D. & Mofrad, M.R.K. (2010). On the multiscale modeling of heart valve biomechanics in health and disease. *Biomechanics and Modeling in Mechanobiology 9*(4): 373–387.